Discovery of a low-mass companion to the F7V star HD 984

T. Meshkat,[1][*] M. Bonnefoy,[2,3] E. E. Mamajek,[4] S. P. Quanz,[5] G. Chauvin,[2,3]
M. A. Kenworthy,[1] J. Rameau,[6] M. R. Meyer,[5] A.-M. Lagrange,[2,3] J. Lannier[2,3]
and P. Delorme[2,3]

[1]*Leiden Observatory, PO Box 9513, Niels Bohrweg 2, NL-2300 RA Leiden, the Netherlands*
[2]*Université Grenoble Alpes, IPAG, F-38000 Grenoble, France*
[3]*CNRS, IPAG, F-38000 Grenoble, France*
[4]*Department of Physics and Astronomy, University of Rochester, Rochester, NY 14627-0171, USA*
[5]*Institute for Astronomy, ETH Zurich, Wolfgang-Pauli-Strasse 27, CH-8093 Zurich, Switzerland*
[6]*Institut pour la Recherche sur les Exoplanètes (iREx), Département de physique, Université de Montréal, C.P. 6128 Succ. Centre-ville, Montréal, QC H3C 3J7, Canada*

ABSTRACT

We report the discovery of a low-mass companion to the nearby ($d = 47$ pc) F7V star HD 984. The companion is detected 0.19 arcsec away from its host star in the L' band with the Apodized Phase Plate on NaCo/Very Large Telescope and was recovered by L'-band non-coronagraphic imaging data taken a few days later. We confirm the companion is comoving with the star with SINFONI integral field spectrograph $H + K$ data. We present the first published data obtained with SINFONI in pupil-tracking mode. HD 984 has been argued to be a kinematic member of the 30 Myr-old Columba group, and its HR diagram position is not altogether inconsistent with being a zero-age main sequence star of this age. By consolidating different age indicators, including isochronal age, coronal X-ray emission, and stellar rotation, we independently estimate a main-sequence age of 115 ± 85 Myr (95 per cent CL) which does not rely on this kinematic association. The mass of directly imaged companions are usually inferred from theoretical evolutionary tracks, which are highly dependent on the age of the star. Based on the age extrema, we demonstrate that with our photometric data alone, the companion's mass is highly uncertain: between 33 and 96 $M_{\rm Jup}$ (0.03–0.09 $M_\odot$) using the COND evolutionary models. We compare the companion's SINFONI spectrum with field dwarf spectra to break this degeneracy. Based on the slope and shape of the spectrum in the H band, we conclude that the companion is an M6.0 $\pm$ 0.5 dwarf. The age of the system is not further constrained by the companion, as M dwarfs are poorly fit on low-mass evolutionary tracks. This discovery emphasizes the importance of obtaining a spectrum to spectral type companions around F-stars.

Key words: techniques: image processing – techniques: high angular resolution – instrumentation: adaptive optics – stars: individual: HD 984 – stars: low-mass.

1 INTRODUCTION

Young stars are the primary targets of exoplanet imaging surveys because associated planets are warm and therefore bright in the infrared. A handful of brown dwarfs and low-mass stellar companions have been found in these surveys (PZ Tel B; Biller et al. 2010, CD-35 2722 B; Wahhaj et al. 2011, HD 1160 B,C; Nielsen et al. 2012). Masses of directly imaged companions are estimated from the companion's luminosity and theoretical evolutionary models, which are very sensitive to the age and distance of the host star.

The companion mass-ratio distribution quantifies the mass ratio of a binary system (Reggiani & Meyer 2013). Based on observational data, the initial mass function for brown dwarfs and very-low-mass-stars (0.08–0.2 $M_\odot$) likely differs from stars (Thies et al. 2015). The primary formation mechanisms for these low-mass companions, including fragmentation and capture, is still under debate, making each new discovered low-mass companion an important test case for the theoretical formation mechanisms of low-mass companion. The orbital motion of the companion around the primary star, measured as a small arc on the sky, can be used to find orbital

[*] E-mail: meshkat@strw.leidenuniv.nl

solutions (Pearce, Wyatt & Kennedy 2015). Some orbital properties, such as eccentricity, can be constrained with only two measurements (Biller et al. 2010). Additionally, with multiple epoch astrometric measurements from direct imaging and radial velocity (RV) data, the dynamical mass of a companion can be measured. This acts as an important comparison with the inferred companion masses from theoretical evolutionary models (Close et al. 2007; Bonnefoy et al. 2009; Dupuy et al. 2015).

We report the detection of a companion around the F7V star HD 984 (HIP 1134). This star has been part of many imaging surveys searching for planets (Rameau et al. 2013; Brandt et al. 2014) due to its proximity, brightness ($d = 47.1 \pm 1.4$ pc; $V = 7.3$; ESA 1997; van Leeuwen 2007), and proposed youth (30 Myr; Zuckerman et al. 2011). However, no comoving companions have yet been reported. Ground-based submm and *Spitzer* infrared photometry of HD 984 have not detected any evidence of a dusty debris disc (Mamajek et al. 2004; Carpenter et al. 2009; Ballering et al. 2013).

In Section 2, we describe our coronagraphic and non-coronagraphic observations with NaCo on the Very Large Telescope (VLT), and our SINFONI/VLT integral field spectrographic data. In Section 3, we measure the companion's photometry and astrometry. In Section 4, we discuss previous age estimates of HD 984, estimate the age of the primary based on its main-sequence isochronal age and other age indicators, and derive the mass of the companion based on evolutionary models and spectral analysis. We conclude in Section 5.

2 OBSERVATIONS

2.1 NaCo/VLT

Observations of HD 984 were taken on UT 2012 July 18 and 20 (089.C-0617(A), PI: Sascha Quanz) at the VLT/UT4 with NaCo (Lenzen et al. 2003; Rousset et al. 2003). The Apodized Phase Plate coronagraph (APP; Kenworthy et al. 2010; Quanz et al. 2010) was used for diffraction suppression thus increasing the chances of detecting a companion very close to the target star. Data were obtained with the L27 camera, in the L'-band filter ($\lambda = 3.80$ μm and $\Delta\lambda = 0.62$ μm). The visible wavefront sensor was used with HD 984 as the natural guide star. We observed in pupil-tracking (PT) mode (Kasper et al. 2009) for Angular Differential Imaging (ADI; Marois et al. 2006). We intentionally saturated the point spread function (PSF) core to increase the signal to noise from potential companions in each exposure. Unsaturated data were also obtained to calibrate photometry relative to the central star.

The APP suppresses diffraction over a 180° wedge on one side of the target star. Excess scattered light is increased on the other side of the target that is not used in the data analysis. Two data sets were obtained with different initial position angles (P.A.) for full 360° coverage around the target star. The field rotation was 47°.4 in the first hemisphere and 42°.5 in the second hemisphere.

Direct imaging observations of HD 984 were obtained on VLT/NaCo on UT 2012 July 20 (089.C-0149(A), PI: Julien Rameau). The data were taken with the L27 camera on NaCo in ADI PT mode. Both the saturated and unsaturated data were imaged in L' band with the same exposure time, but in the unsaturated images a neutral density filter (ND_LONG) was used. The field rotation was 41°.3 in the direct imaging data. All data sets were obtained in cube mode. Each APP cube contains 120 frames, with an integration time of 0.5 s per frame. The total integration time in the APP was 60 min in hemisphere 1 (60 cubes) and 66 min in hemisphere 2 (66 cubes). Unsaturated APP exposures were 0.056 s per frame (222 frames in

12 cubes), with a total time on target of 150 s. The direct imaging cubes contain 100 frames, with 0.2 s per frame, with a total integration time of 48 min for the saturated data and 202 s for the unsaturated data.

A dither pattern on the detector was used to subtract sky background and detector systematics from both data sets, as detailed in Kenworthy et al. (2013). Data cubes are subtracted from each other, centroided and averaged over. Optimized principal component analysis (PCA) is run on both of the APP hemispheres and direct imaging data independently, following Meshkat et al. (2014). Six principal components are used to model the stellar PSF, which results in the highest signal-to-noise detection of the companion. PCA processed frames are derotated and averaged to generate the final image with north facing up.

2.2 SINFONI/VLT

Data were obtained on HD 984 with the AO-fed integral field spectrograph SINFONI (Eisenhauer et al. 2003; Bonnet et al. 2004) at the VLT on UT 2014 September 9 (093.C-0626, PI: G. Chauvin) in ∼0.5 arcsec seeing. The $H + K$ grating was used, which has a resolution of ∼1500. The spatial sampling was 12.5 mas × 25 mas (in the horizontal and vertical directions, respectively) resulting in a field of view of 0.8 arcsec × 0.8 arcsec. We obtained 42 raw cubes of the target, each consisting of 10 × 4 s co-added exposures. Similar to the NaCo observations, data were obtained in PT mode (Hau et al., in preparation). The companion rotated 49°.26 around the centre of the field of view during our 28 min integration.

The instrument pipeline version 2.5.2[1] was used to correct the raw science frames from hot and non-linear pixels, detector gain, and distortion. Final cubes were reconstructed from the resulting frames, associated wavelength map, and slitlet positions. Data cubes were corrected for OH lines and background emission using a dedicated algorithm (Davies 2007) implemented in the pipeline.

The wavelength-dependent drift in the star position, caused by the atmospheric refraction, was registered (modelled by a third-order polynomial) and corrected. We took the mean of the parallactic angle values at the beginning and end of a given exposure, which is stored in the cube file headers. We processed the cubes with the classical-ADI (CADI) algorithm (Marois et al. 2006) to suppress the stellar flux independently at each wavelength (2172 independent spectral resolution elements).

Data were corrected for telluric absorption lines using the observations of an A3V standard star (HD 2811) obtained close in time to HD 984 and at a comparable airmass. The resulting spectrum of HD 984 was flux-calibrated using the 2MASS H-band magnitude of the star (Skrutskie et al. 2006) and a spectrum of Vega.

3 PHOTOMETRY AND ASTROMETRY OF HD 984 B

3.1 NaCo/VLT

The companion was clearly detected very close to the star (Fig. 1, APP hemisphere 1 on top-left and direct imaging on top-right). The companion detection was confirmed using the *Pynpoint* pipeline (Amara & Quanz 2012) and the IPAG-ADI pipeline (Chauvin et al.
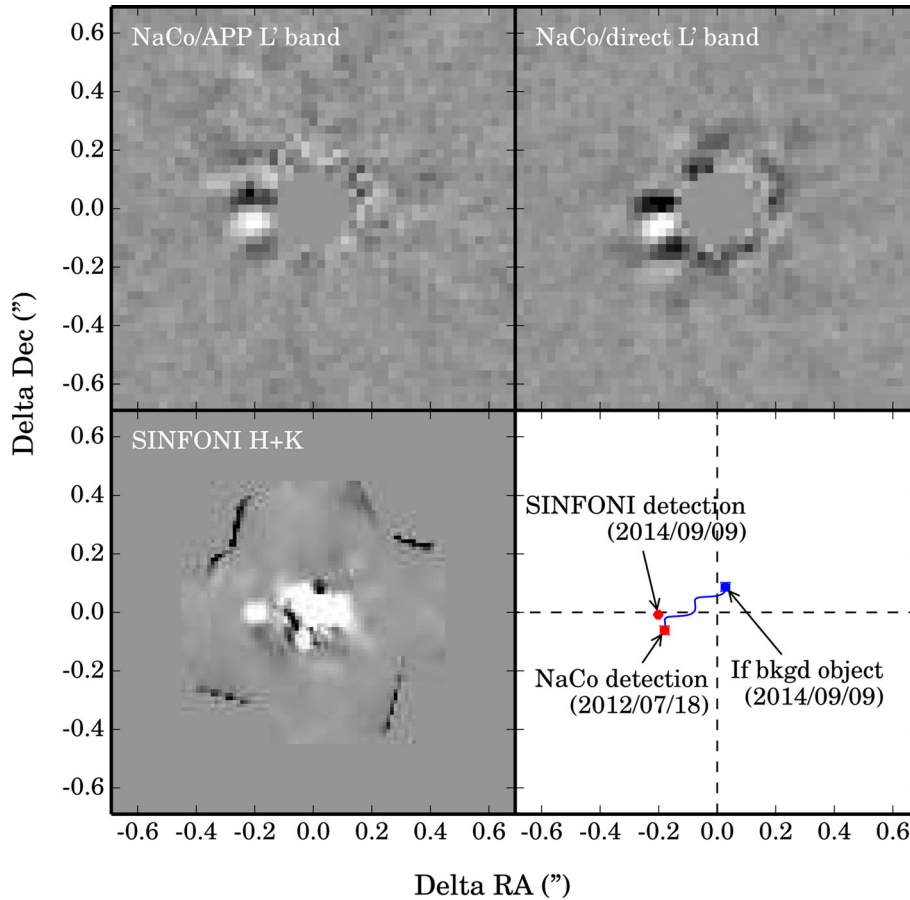
---

[1] http://www.eso.org/sci/software/pipelines/sinfoni/sinfoni-pipe-recipes.html

Figure 1. Top-left: final PCA processed image of HD 984 APP hemisphere 1 data with north facing up. 20 principal components were used to model the stellar PSF in this image. Top-right: final PCA processed image of HD 984 from direct imaging data with north facing up. Six principal components were used to model the stellar PSF. Bottom-left: collapsed $H + K$ SINFONI IFS data cubes processed with CADI, with north facing up. All three images are displayed in the same colour scale. Bottom-right: the position of the companion is plotted as red points for both the VLT/NaCo data set epoch (UT 2012 July 18) and the VLT/SINFONI epoch (UT 2014 September 9). The blue point is the position of the companion if it were a background source at the time of the VLT/SINFONI data set epoch (UT 2014 September 9). Error bars are included for all points.

2012). The detection was robust against changing the number of principal components used in the stellar PSF model.

We used artificial negative companions to determine the astrometry and photometry of the companion (following Meshkat et al. 2015). The unsaturated stellar PSF was used to generate artificial companions in the APP and direct imaging data. A scaling factor of 0.018 was applied to the direct imaging unsaturated data to account for the attenuation from the neutral density filter. We injected artificial negative companions into the data near the expected position of the companion in steps of 0.1 pixels. The artificial companion contrast was varied from 5.0 to 7.0 in steps of 0.01 mag. The chi-squared minimization over the λ/D patch at the location of the artificial negative companion yielded the following results.

Based on this analysis, the companion contrast in the APP data is best approximated as $\Delta L' = 6.0 \pm 0.2$ mag ($L' = 12.0 \pm 0.2$ mag). The angular separation of the companion is 0.19 ± 0.02 arcsec, which corresponds to a projected separation of 9.0 ± 1.0 au for the stellar distance of 47.1 ± 1.4 pc from van Leeuwen (2007). The position angle (P.A.) of the companion is $108°8 \pm 3°0$. The error in the measurements is due to the range in artificial companions which successfully subtract the companion signal.

The companion contrast in the direct imaging data is $\Delta L' = 5.9 \pm 0.3$ mag at 0.208 ± 0.023 arcsec (9.8 ± 1.1 au). The P.A. of the companion is $108°9 \pm 3°1$ corrected to true north orientation, calibrated using θ Ori, observed at the same epoch with the same mode. The θ Ori stars TCC058, 057, 054, 034, and 026 were used to determine the true north $0°41 \pm 0°07$ with a plate scale of 27.11 $\pm$ 0.02 mas (Rameau et al. 2013). The astrometry and photometry of the companion is in good agreement between the two data sets. Since the two data sets were only taken two days apart, we do not consider them separate epochs, but rather a confirmation that this companion is not an artefact.

3.2 SINFONI

The companion was detected in $H + K$ band integral field spectrograph (IFS) SINFONI data (Fig. 1 bottom-left). These data are the first published results demonstrating the capabilities of the SINFONI instrument in PT mode. The parallactic angle associated with each of the 43 data cubes was estimated by taking the mean of the parallactic angle at the beginning and the end of an exposure. We applied an additional clockwise rotation of $210°92$ to the frames at the ADI reduction step to properly realign the field of view to the north.

True north was estimated using GQ Lup SINFONI observations on UT 2013 August 24, which were calibrated with NaCo observations of the same source on UT 2012 March 3, assuming orbital motion is negligible between the epochs (following the formulae described in the appendix).

The companion is detected in all of our ADI analyses. We discovered that subtracting the stellar halo of the data cubes collapsed in wavelength followed by a realignment of the frame to the north also allowed detection of the companion. Unlike ADI processing, this allows for a measurement of the position of the companion without the biases associated with the self-subtraction of the companion PSF (Bonnefoy et al. 2011). We selected 10 frames corresponding to the first 10 cubes of the PT sequence and median-combined them after realigning to true north. This provided a good removal of residual speckles from the stellar halo. We found that HD 984 B lies at a PA = $92°.2 \pm 0°.5$ and a separation $\rho = 201.6 \pm 0.4$ mas. The error considers uncertainties in our fitting function as well as true north. We also make the assumption that the instrument absolute orientation on sky did not vary between our UT 2014 September 9 observations and the true north calibration (UT 2013 August 24) with GQ Lup. The separation assumes a plate scale of 12.5 mas pixel^{-1} reported in the instrument user manual. The plate scale at the time of HD 984 observations could not be measured.

HD 984 is a relatively high proper motion star, with $\mu_{\alpha*}$, μ_δ = 102.79 ± 0.78, -66.36 ± 0.36 mas yr^{-1} (van Leeuwen 2007). If the companion were a background source, it should be due north of HD 984 and at a projected separation of <0.1 arcsec in the SINFONI data (Fig. 1, bottom-right). We estimate that the companion is very unlikely to be a stationary background source, with an estimated χ^2 probability of less than 10^{-6} based on the two epoch companion detections, stellar proper motion, distance estimates, and the astrometric error on the SINFONI data set (which is dependent on the plate scale). The new P.A. of the companion is consistent with Keplerian orbital motion. Based on the astrometry of the companion, we confirm it is bound to the star and not a background object.

The companion flux was integrated in a 6 pixel wide circular aperture in the processed CADI cubes to generate the spectrum. We applied the same procedure to HD 984. We corrected for flux losses in the companion's spectrum (caused by the image processing algorithms) by adding artificial sources. We used the unsaturated primary star itself to scale and inject artificial sources in the data. Artificial sources were added in each wavelength at the same projected separation as the companion, but with a P.A. difference of $-90°$, $+90°$, and $+180°$. The resulting spectrum was corrected for the telluric lines using the primary spectrum. We obtained the final flux-calibrated spectrum of the companion by multiplying the flux ratio between the system components and the flux-calibrated spectrum of the star. Based on the flux ratio between HD 984 and B in H and Ks band, we estimate $H_{2MASS} = 12.58 \pm 0.05$ mag and $Ks_{2MASS} = 12.19 \pm 0.04$ mag for the companion. The spectrum of the companion is analysed in Section 4.2.

Fig. 2 shows contrast curves comparing the sensitivity to point sources in the data processed with the CADI algorithm in H and Ks band. The contrast curve was generated following Chauvin et al. (2015). We injected fake planets every 10 pixels radially at P.A.s of $0°$, $120°$, and $240°$ between 125 and 375 mas, in order to correct for flux losses. The fake planets are created by scaling the flux of the primary star. We created a pixel-to-pixel noise map by sliding a box of 5×5 pixels from the star to the limit of the SINFONI field of view. The 5σ detection limit is found by dividing the pixel-to-pixel noise map by the flux loss, taking into account the relative calibration between the fake planet and the primary star.
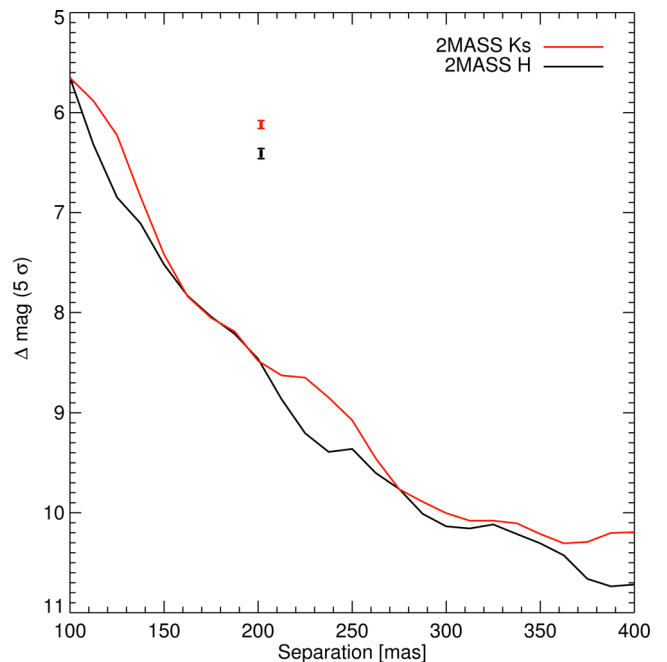

Figure 2. Contrast curves for the SINFONI HD 984 H (black curve) and Ks (red curve) data, for CADI processing. The companion detection is shown as a point with error bars in H (black) and Ks (red), respectively.

4 ANALYSIS

4.1 Primary Star HD 984

HD 984 is a $V = 7.32$ mag (ESA 1997) F7V star (Houk & Swift 1999) at a distance of 47.1 ± 1.4 pc (van Leeuwen 2007, $\varpi = 21.21 \pm 0.64$ mas). The star has colour $B-V = 0.522 \pm 0.010$ from the Tycho catalogue (ESA 1997), and for its calculated absolute magnitude ($M_V = 3.95 \pm 0.07$) the star lies squarely on the field star main sequence of Wright et al. (2004), which predicts M_V(MS) $\simeq 3.95$ for this $B-V$ colour. It is not listed in latest version[2] of the Washington Double Star catalogue (Mason et al. 2001). The interstellar reddening and extinction towards HD 984 is likely to be negligible as it lies within the Local Bubble (e.g. Reis et al. 2011). Examining the reddening estimates for 19 stars in the catalogue of Reis et al. (2011) that have Galactic longitude within $\pm20°$ of HD 984 and latitude $b < -48°$ (their survey only extends to $b = -60°$), we find no stars within 60 pc that have a $E(b-y)$ reddening that exceeds 1σ from zero. Indeed, a fit of distance versus $E(b-y)$ reddening for the 19 stars in this region of sky with $d < 150$ pc is consistent with negligible reddening ($E(b-y) \simeq d_{pc} \times 0.01$ mmag). Given this trend, for a star at $d \simeq 47$ pc, one would expect reddening of $E(b-y) \simeq 2$ mmag and extinction $A_V \simeq 0.01$, i.e. utterly negligible compared to our photometric uncertainties. Based on this, we assume negligible reddening or extinction for HD 984 and its companion.

Numerous estimates of the effective temperature have been reported (e.g. Valenti & Fischer 2005; Masana, Jordi & Ribas 2006; Schröder, Reiners & Schmitt 2009; Casagrande et al. 2011). We adopt the recent value from Casagrande et al. (2011) (6315 ± 89 K), which is also close to the median value among recent published estimates. From fitting the optical–infrared photometry to the dwarf
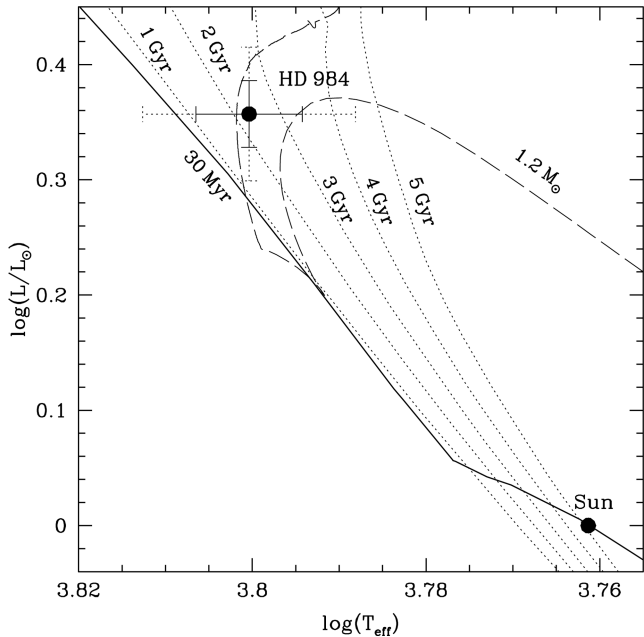
Figure 3. HR diagram position of HD 984 and the Sun, with isochrones and evolutionary tracks from Bressan et al. (2012) overlaid ($z = 0.017$), with 1σ solid line and 2σ dotted line error bars. The solid line is a 30 Myr isochrone corresponding to the purported age of the Columba group. Dotted lines are isochrones with ages of 1, 2, 3, 4, 5 Gyr. The dashed line is a 1.20 ± 0.06 (95 per cent CL) M$_\odot$ track.

colour sequences from Pecaut & Mamajek (2013), we derive an apparent bolometric magnitude of HD 984 to be $m_{bol} = 7.257 \pm 0.01$ and bolometric flux[3] of 31.94 ± 0.29 pW m^{-2}. Employing the van Leeuwen (2007) parallax, this bolometric flux translates to a luminosity of $\log(L/L_\odot) = 0.346 \pm 0.027$ dex. Adopting the Casagrande et al. (2011) T_{eff}, this is consistent with a stellar radius of 1.247 ± 0.053 R$_\odot$.

4.1.1 Previous age estimates

Zuckerman et al. (2011), Malo et al. (2013), and Brandt et al. (2014) consider HD 984 to be a member of the Columba group with an age of 30 Myr (Torres et al. 2008). Malo et al. (2013) has demonstrated that HD 984 appears to be comoving with the Columba group. However, there remains the possibility that HD 984 could be a kinematic interloper or that the Columba group is not sufficiently characterized to reliably assign ages based on kinematic membership. Isochronal ages of <0.48 Gyr (68 per cent CL; Takeda et al. 2007), $1.2^{+0.7}_{-0.9}$ Gyr (Valenti & Fischer 2005), and $3.1^{+1.0}_{-1.6}$ Gyr (Holmberg, Nordström & Andersen 2009) have been estimated.

4.1.2 Isochronal age

The HR diagram position of HD 984 is plotted in Fig. 3 along with isochrones from Bressan et al. (2012) (for $Z = 0.017$). HD 984 is a main-sequence star, and any derived isochronal age will have large uncertainties. Simulating the HR diagram position and interpolating their ages and masses, the isochronal ages are consistent with $2.0^{+2.1}_{-1.8}$

[3] Our F_{bol} value is within 3.5 per cent of that of Casagrande et al. (2011): 30.824 pW m^{-2}.

(95 per cent CL) Gyr and 1.20 ± 0.06 (95 per cent CL) M$_\odot$ (dashed line). However, as Fig. 3 shows, a 2σ deviation (dashed error bar line) in both T_{eff} and $\log(L/L_\odot)$ are consistent with the 30 Myr isochrone. It takes a 1.2 M$_\odot$ star 27 Myr to reach the main sequence, and ages of $\lesssim 30$ Myr can be ruled out based on the isochronal age constraints for the secondary HD 984 B (see Section 4.2). Based on the HR diagram position of HD 984 compared to stellar evolutionary tracks and isochrones, we deduce that the isochronal age of HD 984 is likely between ~30 Myr (zero-age main sequence) and ~4 Gyr.

4.1.3 Other age indicators

We examine other age diagnostics for HD 984 to help constrain its age. HD 984 appears to be fairly chromospherically and coronally active, which hint at fast rotation and youth. Wright et al. (2004) estimated an age for HD 984 of 0.49 Gyr based on chromospheric activity. The star has mass ~1.2 M$_\odot$, $B-V \simeq 0.52$, and $T_{eff} \simeq$ 6300 K, which corresponds almost exactly with the 'Kraft break' (Kraft 1967; Angus et al. 2015). This region divides F-type stars with thin convective envelopes, mostly radiative interiors with small convective cores, and which slow down less efficiently during their main-sequence phases, from solar-type stars with thicker convective envelopes, radiative cores, and which slow down appreciably during their main-sequence phase. The gyrochronology relations are not well constrained near the Kraft break (e.g. Mamajek & Hillenbrand 2008) – and may not be applicable. We can, however, quantify just how active HD 984 is compared to nearby stars of similar spectral type.

Coronal X-ray and chromospheric Ca H&K emission: HD 984 has an X-ray counterpart (1RXS J001410.1-071200) in the *ROSAT* All-Sky Survey Bright Source Catalogue (Voges et al. 1999). The X-ray source is 4 arcsec away from the optical position, but with position error of 8 arcsec, the match with HD 984 is highly probable. Based on the *ROSAT* X-ray count rate (0.265 ± 0.029 ct s^{-1}) and hardness ratio HR1 (HR1 $= -0.20 \pm 0.10$), and using the formulae in Fleming, Schmitt & Giampapa (1995) and Mamajek & Hillenbrand (2008), we estimate the following properties: 0.1–2.4 keV X-ray flux $f_X = 1.92 \times 10^{-12}$ erg s^{-1} cm^{-2}, $\log(L_X/\text{erg s}^{-1}) = 29.71$ dex, and $\log(L_X/L_{bol}) = -4.22$ dex. It is unlikely that the X-ray emission is from the low-mass companion alone as the star would have to be emitting ~40 times more powerful than that predicted for saturated X-ray emission ($\log(L_X/L_{bol})$, so the primary is almost certainly completely dominating the X-ray flux. Among nearby F-type dwarfs in the *ROSAT* study of Hünsch et al. (1999), the mean relation of coronal X-ray activity values goes as $\log(L_X/L_{bol})$ $\simeq -6.60 + 2.67(B-V)$, with rms scatter ± 0.68 dex. HD 984 is 0.98 dex (~1.4σ) brighter in $\log(L_X/L_{bol})$ than this locus and suggestive that the star is amongst the most active ~4 per cent of F-type dwarfs.

Based just on the coronal X-ray emission ($\log(L_X/L_{bol} = -4.22$ dex), one would predict strong chromospheric activity $\log(R'_{HK})$ $\simeq -4.34$ using equation A1 of Mamajek & Hillenbrand (2008). Indeed, this predicted $\log(R'_{HK})$ is close to that reported from multiple surveys – $\log(R'_{HK})$ ranges from -4.31 (Schröder et al. 2009) to -4.46 (Pace 2013), with a mean value of approximately -4.40 (Wright et al. 2004; White, Gabor & Hillenbrand 2007; Schröder, Reiners & Schmitt 2009; Isaacson & Fischer 2010; Pace 2013). In a catalogue of unique FGK stars with $\log(R'_{HK})$ values from the surveys of Henry et al. (1996), Wright et al. (2004), and Gray et al. (2006), one finds 146 single main-sequence *Hipparcos* stars with $B-V$ within ± 0.02 mag of HD 984's colour (0.52). Among these dwarf stars of similar colour to HD 984, its $\log(R'_{HK})$ value

(∼−4.40) places it among the most chromospherically active 5 per cent, similar to that inferred from the coronal activity. The star's combination of colour ($B-V = 0.52$) and chromospheric activity ($\log(R'_{HK}) \simeq -4.40$) for HD 984 can also be compared to stars to various samples in fig. 4 of Mamajek & Hillenbrand (2008): Sco–Cen (∼0.01–0.02 Gyr), the Pleiades (∼0.13 Gyr), the Hyades (∼0.6 Gyr), the M67 cluster (∼4 Gyr), and field stars. The star's chromospheric activity is less active than typical Sco–Cen members, most consistent with the Pleiades locus, would be near the upper limit of that seen among Hyades members, and is way more active than M67 members and the median values calculated for late F-type stars.

Rotation: given the star's projected rotational velocity ($v\sin i = 42.13 \pm 1.65$ km s^{-1}; White et al. 2007) and the calculated radius (1.247 ± 0.053 R$_{\odot}$), this implies that the star's rotation period must be P$_{\rm rot} < 1.5$ d. Note that among 487 stars classified as F7 dwarfs in the Głębocki & Gnaciński (2005) compendium of projected rotational velocities ($v\sin i$), HD 984 is among the top ∼1 per cent fastest rotating stars. The F7 dwarfs in the Głębocki & Gnaciński (2005) catalogue have median $v\sin i \simeq 7.2$ km s^{-1} with 95 per cent range of 2.7–35.2 km s^{-1}. The mean $v\sin i$ value for a F7 star of similar colour and absolute magnitude to HD 984 in the ∼0.6 Gyr-old Hyades cluster is approximately 12 km s^{-1}, and none within ±0.05 mag in $B-V$ of HD 984 have $v\sin i > 20$ km s^{-1} (Soderblom et al. 1993). In the Pleiades, however, there are stars of similar colour to HD 984 with $v\sin i$ of ∼40–60 km s^{-1} (Soderblom et al. 1993). The star's combination of $\log(L_X/L_{\rm bol})$ and $v\sin i$ for its $V-I$ colour (0.59; ESA 1997) appears typical among F-type stars in the ∼50 Myr-old IC 2391 and IC 2602 clusters, and would place it among the fastest rotators in the ∼130 Myr-old Pleiades (see fig. 6 of Stauffer et al. 1997), where the quoted ages are Li-depletion ages from Barrado y Navascués, Stauffer & Jayawardhana (2004) and Dobbie, Lodieu & Sharp (2010).

The rotation, coronal activity, and chromospheric activity indicators for HD 984 seem consistent with a very young, active main-sequence star. The rotation and X-ray emission are consistent with the star being amongst the youngest ∼1–5 per cent of F7 dwarfs. The main-sequence lifetimes of ∼1.2 M$_{\odot}$ stars are ∼5 Gyr (Bressan et al. 2012), suggesting that if HD 984 is amongst the youngest ∼1–4 per cent of F7 dwarfs, that its age is very likely to be ≲200 Myr. This would be consistent with its chromospheric activity being similar to that of Pleiades members, its rotation being similar to that of ∼50 Myr stars in IC 2391 and IC 2602 (although near the upper limit of projected rotation velocities for Pleiades members), and its rotation and activity indicators all being very inconsistent with Hyades-age stars. Based on rotation and activity indicators, we adopt a strong upper limit on the age of HD 984 of <200 Myr. The fact that the star is on the main sequence places an approximate lower limit of 30 Myr. We conclude that an approximate age for the primary star HD 984 that is independent of any kinematic membership or consideration of the properties of the secondary is 30–200 Myr (95 per cent CL).

4.2 Companion characteristics

Based on the NaCo L' photometry alone, the companion mass can only be estimated from theoretical models which are highly dependent on the age of the star and lead to large uncertainties in the determined mass. Using the COND evolutionary tracks (Baraffe et al. 2003), if the system is 30 Myr, the companion may be a $33 \pm 6 M_{\rm Jup}$ young brown dwarf. If the system is 200 Myr, the companion may be a 0.09 ± 0.01 M$_{\odot}$ low-mass star, likely an M5–M6
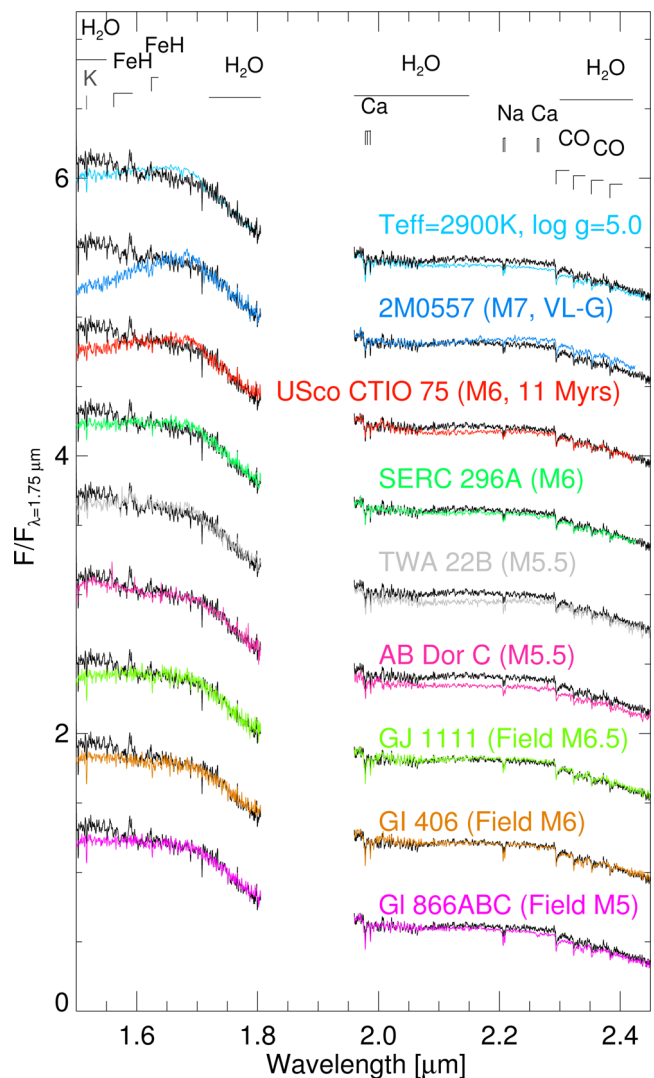

Figure 4. Comparison of HD 984 B spectrum (black) to those of field dwarfs, young companions, isolated objects, and to the best-fitting BT-COND spectrum. It enables us to conclude that HD 984 B is an M6.0 ± 0.5 dwarf.

dwarf. The errors are based on the uncertainty in the photometry and the distance of the star and do not include systematic uncertainties in the models. The range of companion masses based on the DUSTY evolutionary model (Chabrier et al. 2000) is within the errors of the values derived from the COND model: 30 Myr and $34 \pm 6 M_{\rm Jup}$ or 200 Myr and 0.10 ± 0.01 M$_{\odot}$. Thus, the companion mass estimation based on photometry is not significantly impacted by the evolutionary model chosen.

We compare our CADI analysis of the SINFONI spectrum (black spectrum, see Fig. 4) with field dwarfs from the IRTF library (Cushing et al. 2005; Rayner, Cushing & Vacca 2009). We perform a least-squares fit of the spectra to determine the best fit. In addition to the overall spectral slope from 1.5 to 2.45 µm, we aim to fit the following spectral features: the K I band at 1.516 µm, the Ca I triplet near 1.98 µm, the Na I doublet near 2.207 µm, the CO overtones longwards of 2.3 µm, and the overall shape of the *Ks* band which is sensitive to the collision-induced absorption of molecular hydrogen, thus to the atmospheric pressure and surface gravity. The companion has features later than M5 and midway between those

of M5.5 and M6.5 field dwarfs. The SINFONI spectra of the young (≤ 150 Myr) mid-M companions AB Dor C and TWA 22 B (Close et al. 2007; Bonnefoy et al. 2009) reproduce the pseudo-continuum in the H band, but have bluer slopes than our companion, suggesting a later spectral type for HD 984 B. Spectra of other young mid-M dwarfs have a more triangular H-band shape than our object. The companion fits well with the M6 object SERC 296A (Thackrah, Jones & Hawkins 1997; Allers & Liu 2013), which does not appear to be a good candidate member to any nearby associations based on its kinematics (Gagné et al. 2014), but has an age below $\sim$200 Myr due to lithium absorption. We therefore conclude that the HD 984 B is more likely a M6.0 $\pm$ 0.5 object, which is younger than the typical field dwarf age ($\gg$1 Gyr). The subtype accuracy is due to the companion features being intermediate between a M5.5 and an M6.5.

The spectral type of M6.0 $\pm$ 0.5 corresponds to $T_{\text{eff}} = 2777^{+127}_{-130}$ K using the conversion scale of Stephens et al. (2009). The T_{eff} accuracy is the quadratic combination of the spectral type estimate and systematic uncertainty. Conversely, the companion's pseudo-continuum shape and main absorption features are best reproduced by BT-COND and *GAIA* synthetic spectra (Brott & Hauschildt 2005; Allard et al. 2013) with $T_{\text{eff}} = 2900 \pm 200$ K and log $g = 5.0$–5.5 dex. The accuracy on T_{eff} is limited by the intrinsic differences and uncertainties between the atmospheric model grids (H band is known to be badly reproduced by models, see Bonnefoy et al. 2013). Rajpurohit et al. (2013) find a T_{eff} range of 2700–3000 K for M5.5–M6.5 dwarfs by fitting BT-Settl (Allard et al. 2013) spectra to optical spectra of M dwarfs. This is consistent with our spectral type and derived temperature.

We calculate the bolometric luminosity based on our derived spectral type and H, Ks, and L'-band companion magnitude measurements. We adopt bolometric corrections of $BC_{H(B)} = 2.588 \pm 0.032$ mag, $BC_{Ks(B)} = 2.940 \pm -0.015$ mag, and $BC_{L'(B)} = 3.260 \pm 0.022$ mag by interpolating between an M6 and M7 dwarf, using bolometric correction and colour information for M dwarfs from Pecaut & Mamajek (2013), Schmidt et al. (2014), and Dupuy & Liu (2012). By taking the weighted mean of our bolometric luminosity calculations from H, Ks and L'-band measurements, we find log($L/L_\odot$) = -2.815 ± 0.024 dex. These results are summarized in Table 1.

Fig. 5 compares the derived T_{eff} of the companion against the BHAC15 (Baraffe et al. 2015) evolutionary tracks of different ages. Comparing our derived bolometric luminosity with evolutionary tracks suggests that the companion is consistent with our derived stellar age of 115 $\pm$ 85 Myr. HD 984 B demonstrates the challenges in fitting M dwarfs on low-mass evolutionary tracks. Thus, we can rule out ages less than 30 Myr based on the companion HR diagram position and we have demonstrated that this companion is consistent with an M6.0 $\pm$ 0.5 object.

Recently, Hinkley et al. (2015) announced the detection of seven companions with short projected separations around intermediate mass stars in the Scorpius–Centaurus association. HD 984 B has a companion-to-star mass ratio of $0.067^{+0.028}_{-0.035}$ based on the mass derived from the luminosity. Given the small separation of the system (9.5 au), HD 984 B shares similar characteristics as the aforementioned companions discovered by Hinkley et al. (2015).

5 CONCLUSION

We report the discovery of a low-mass companion to the F7V star HD 984. This companion was detected in L' band with the APP coronagraph and non-coronagraphic photometry with the NaCo in-

Table 1. System properties.

Property	HD 984	HD 984 B
Distance (pc)[a]	47.1 $\pm$ 1.4	
Age (Myr)[b]	30–200	
A_V[c]	0	
T_{eff}	6315 $\pm$ 89	$2777^{+127\,d}_{-130}$
		2900 $\pm$ 200[e]
Spectral type	F7V	M6.0 $\pm$ 0.5
log($L/L_\odot$)	0.36 $\pm$ 0.03	-2.815 ± 0.024
Mass	1.20 $\pm$ 0.06 M$_\odot$	74^{+27}_{-31} M_{Jup}[d]
		90^{+69}_{-42} M_{Jup}[e]
		84^{+29}_{-42} M_{Jup}[f]
Separation (mas)	201.6 $\pm$ 0.4	
P.A.(°)	92.2 $\pm$ 0.5	
H	6.170 $\pm$ 0.023	12.58 $\pm$ 0.05
Ks	6.073 $\pm$ 0.038	12.19 $\pm$ 0.04
L'	6.0 $\pm$ 0.1	12.0 $\pm$ 0.2

Notes. [a]*Hipparcos* catalogue (van Leeuwen 2007).
[b]This work.
[c]Schlegel, Finkbeiner & Davis (1998) and Reis et al. (2011).
[d]Based on the spectral type conversion scale of Stephens et al. (2009).
[e]Based on BT-COND and GAIA synthetic spectra.
[f]Converted from the derived log($L/L_\odot$) for HD 984 B.
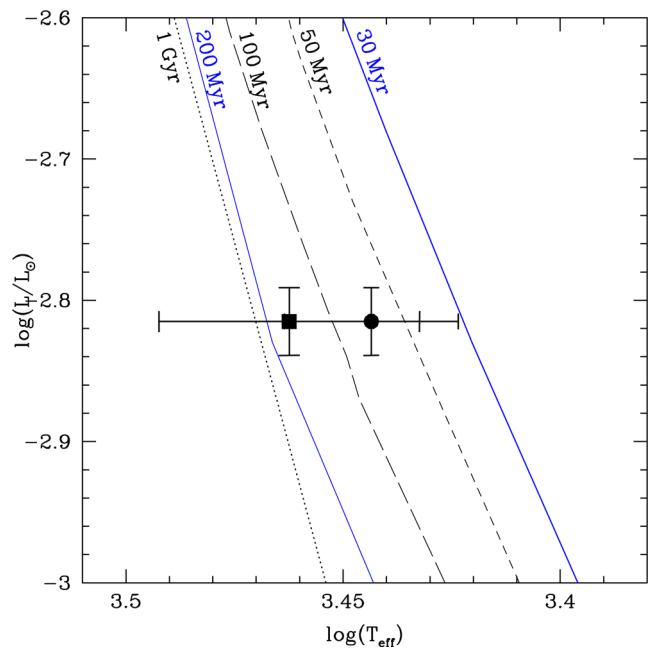

Figure 5. HR diagram position of HD 984 B in bolometric luminosity (right) based on our spectral type estimate and adopting the Stephens et al. (2009) T_{eff} scale (circle), BT-COND and *GAIA* synthetic spectra (Brott & Hauschildt 2005; Allard et al. 2013: square). The BHAC15 (Baraffe et al. 2015) evolutionary tracks are plotted for 30, 50, 100, 200 Myr, and 1 Gyr. The 30 and 200 Myr isochrones are in blue to indicate the consistency with the lower and upper age limits determined in this work.

strument on the VLT. HD 984 has been reported to be part of the 30 Myr old Columba association. However, based on our independent analysis of several age indicators, we estimate a main-sequence age of 115 $\pm$ 85 Myr (95 per cent CL). Due to the age uncertainty, the companion mass may range from a low-mass brown dwarf ($\sim$33

$M_{\rm Jup}$) to an M dwarf ($\sim$0.09 M$_\odot$), using the COND evolutionary models.

We analyse the slope and shape of SINFONI $H + K$ IFU data of the companion compared with field M dwarfs. We conclude the companion is an M6.0 $\pm$ 0.5 dwarf. Using our derived spectral type, we aim to determine the age of the system by placing the companion L'-band absolute magnitude and bolometric luminosity on COND evolutionary tracks. While the L'-band HR diagram position allows us to rule out an age less than 50 Myr, the companion's bolometric luminosity position is consistent with an age of $\geq$30 Myr. Thus, we cannot set age constraints on the companion, due to this discrepancy between the companion's position on evolutionary tracks. Future observations in J band could help to look for signatures of low surface gravity in HD 984 B.

Given its small projected separation of just $\sim$9 au, HD 984 B will show significant orbital motion over the next few years, allowing the potential for dynamical mass determination. In order to determine the individual mass components of the HD 984 system, RV data must be obtained. Using the current projected separation as an approximation for the semimajor axis and assuming a circular orbit, we would expect to detect a maximum semi-amplitude from RV of 1.01 km s^{-1} for an M dwarf companion and 0.27 km s^{-1} for a brown dwarf. This calculation assumes the orbit is edge-on ($i = 90°$), however based on our two epoch astrometric measurements, its orbit is unlikely to be edge-on. Even if the companion is closer to face-on ($i = 5°$), the semi-amplitude of 0.087 km s^{-1} for an M dwarf and 0.024 km s^{-1} for a brown dwarf is within the detection limits of RV. This system is also a promising target for *GAIA*, which could reveal the reflex motion of the star and assess the dynamical mass of the companion. These measurements are amplified if the system is face-on, complementing the RV method. Thus, the dynamical mass of this companion can be achieved with RV and astrometric measurements, providing a crucial comparison with the theoretical evolutionary models for mass determination.

We have demonstrated that, given the difficulty in deriving a reliable age for HD 984 that is independent of its purported group membership, the derived colour and spectral parameters of the companion are necessary to determine the companion mass. These results suggest that caution should be used when estimating the masses of companions based on photometric data and stellar age based on kinematic group membership alone. It reinforces the importance of future near-infrared high contrast integral field spectrographs to the characterization of low-mass stellar and substellar companions.

ACKNOWLEDGEMENTS

APPENDIX A: SINFONI ORIENTATION

We calibrated the absolute orientation of the field of view of SINFONI using observations of GQ Lup B from UT 2013 August 24 (technical programme ID 60.A-9800). These observations were obtained using the pre-optics offering a 50 × 100 mas sampling in the $H + K$ band. During the 54 min PT sequence, 100 × 7 s integrations were recorded. The field rotated by 12°.84. We reduced these data following the same procedure as HD 984 B. Once the cubes were corrected for atmospheric refraction, we removed the halo from the primary star centred in the field of view with a radial profile.

We found that a clockwise rotation by the ADA.POSANG + C values of each data cubes re-aligned the final GQ Lup data cubes with the north. ADA.POSANG is a variable found in the image header, corresponding to the position angle of the rotator at the Cassegrain focus at the time of the observations. C is an additional offset related to the calibration of the instrument rotator true north position.

We define ROT.PT.OFF + C = 180° + ADA.PUPILPOS + C, the angular offset needed to realign the frames to the north when the parallactic angle is 0. ADA.PUPILPOS is a keyword stored into the file header, which depends on the telescope pointing position and time of observation. It is redefined at the beginning of any PT sequence, but it remains constant during a PT observing sequence.

We verified that this relation remains valid for other data sets obtained in PT mode on GQ Lup during the same night, on AB Dor C (UT 2013 October 17, 60.A-9800), and on HD 984 B (UT 2014 October 10, 2014 December 3,5,8 094.C-0719), and of the astrometric binary HD 179058 AB (UT 2014 April 26, 60.A-9800). We note that we could not use the observations of the HD 179058 AB to properly calibrate the instrument plate scale and absolute orientation since the binary had likely moved on its orbit since its latest independent astrometric measurement (Tokovinin, Mason & Hartkopf 2010).

For the case of GQ Lup B, the ADA.PUPILPOS keyword was fixed to −0.072 97. Therefore, we adopted ROT.PT.OFF = 179.927. We estimated a value of C = 0°.0 ± 0°.5 comparing the resulting position angle in the derotated cubes to the position angle of the system measured from VLT/NaCo data obtained on 2012 March 3 and reported in Ginski et al. (2014). We note that this value of C assumes that the companion did not have significant orbital motion in the course of one year. This is reasonable given the available VLT/NaCo astrometry of the system recorded since 2008 (see table 2 of Ginski et al. 2014). We also deduce from the SINFONI data of GQ Lup B that the mean square plate scale is 49.30 ± 0.14 mas spaxel^{-1} when the 50 × 100 mas and $H + K$ band mode of the instrument are chosen.

REFERENCES

Allard F., Homeier D., Freytag B., Schaffenberger W., Rajpurohit A. S., 2013, Mem. Soc. Astron. Ital. Suppl., 24, 128
Allers K. N., Liu M. C., 2013, ApJ, 772, 79
Amara A., Quanz S. P., 2012, MNRAS, 427, 948
Angus R., Aigrain S., Foreman-Mackey D., McQuillan A., 2015, MNRAS, 450, 1787
Ballering N. P., Rieke G. H., Su K. Y. L., Montiel E., 2013, ApJ, 775, 55
Baraffe I., Chabrier G., Barman T. S., Allard F., Hauschildt P. H., 2003, A&A, 402, 701
Baraffe I., Homeier D., Allard F., Chabrier G., 2015, A&A, 577, 42
Barrado y Navascués D., Stauffer J. R., Jayawardhana R., 2004, ApJ, 614, 386
Biller B. A. et al., 2010, ApJ, 720, L82

Bonnefoy M. et al., 2009, A&A, 506, 799
Bonnefoy M. et al., 2011, A&A, 528, L15
Bonnefoy M. et al., 2013, A&A, 555, A107
Bonnet H. et al., 2004, The Messenger, 117, 17
Brandt T. D. et al., 2014, ApJ, 794, 159
Bressan A., Marigo P., Girardi L., Salasnich B., Dal Cero C., Rubele S., Nanni A., 2012, MNRAS, 427, 127
Brott I., Hauschildt P. H., 2005, in Turon C., O'Flaherty K. S., Perryman M. A. C., eds, ESA SP-576: The Three-Dimensional Universe with Gaia. ESA, Noordwijk, p. 565
Carpenter J. M. et al., 2009, ApJS, 181, 197
Casagrande L. et al., 2011, A&A, 530, A138
Chabrier G., Baraffe I., Allard F., Hauschildt P., 2000, ApJ, 542, 464
Chauvin G. et al., 2012, A&A, 548, A33
Chauvin G. et al., 2015, A&A, 573, A127
Close L. M., Thatte N., Nielsen E. L., Abuter R., Clarke F., Tecza M., 2007, ApJ, 665, 736
Cushing M. C., Rayner J. T., Vacca W. D., 2005, ApJ, 623, 1115
Davies R. I., 2007, MNRAS, 375, 1099
Dobbie P. D., Lodieu N., Sharp R. G., 2010, MNRAS, 409, 1002
Dupuy T. J., Liu M. C., 2012, ApJS, 201, 19
Dupuy T. J., Liu M. C., Leggett S. K., Ireland M. J., Chiu K., Golimowski D. A., 2015, ApJ, 805, 56
Eisenhauer F. et al., 2003, in Iye M., Moorwood A. F. M., eds, Proc. SPIE Conf. Ser. Vol. 4841, Instrument Design and Performance for Optical/Infrared Ground-based Telescopes. SPIE, Bellingham, p. 1548
ESA, 1997, ESA Special Publication. 1200
Fleming T. A., Schmitt J. H. M. M., Giampapa M. S., 1995, ApJ, 450, 401
Gagné J., Lafrenière D., Doyon R., Malo L., Artigau É., 2014, ApJ, 783, 121
Ginski C., Schmidt T. O. B., Mugrauer M., Neuhäuser R., Vogt N., Errmann R., Berndt A., 2014, MNRAS, 444, 2280
Głębocki R., Gnaciński P., 2005, in Favata F., Hussain G. A. J., Battrick B., eds, ESA SP-560: 13th Cambridge Workshop on Cool Stars, Stellar Systems and the Sun. ESA, Noordwijk, p. 571
Gray R. O., Corbally C. J., Garrison R. F., McFadden M. T., Bubar E. J., McGahee C. E., O'Donoghue A. A., Knox E. R., 2006, AJ, 132, 161
Henry T. J., Soderblom D. R., Donahue R. A., Baliunas S. L., 1996, AJ, 111, 439
Hinkley S. et al., 2015, ApJ, 806, 9
Holmberg J., Nordström B., Andersen J., 2009, A&A, 501, 941
Houk N., Swift C., 1999, Michigan Catalogue of Two-dimensional Spectral Types for the HD Stars, Vol. 5. University of Michigan Press, Ann Arbor, MI
Hünsch M., Schmitt J. H. M. M., Sterzik M. F., Voges W., 1999, A&AS, 135, 319
Isaacson H., Fischer D., 2010, ApJ, 725, 875
Kasper M., Amico P., Pompei E., Ageorges N., Apai D., Argomedo J., Kornweibel N., Lidman C., 2009, The Messenger, 137, 8
Kenworthy M. A., Quanz S. P., Meyer M. R., Kasper M. E., Lenzen R., Codona J. L., Girard J. H., Hinz P. M., 2010, in McLean I. S., Ramsay S. K., Takami H., eds, Proc. SPIE Conf. Ser. Vol. 7735, Ground-Based and Airborne Instrumentation for Astronomy III. SPIE, Bellingham, p. 773532
Kenworthy M. A., Meshkat T., Quanz S. P., Girard J. H., Meyer M. R., Kasper M., 2013, ApJ, 764, 7
Kraft R. P., 1967, ApJ, 150, 551
Lenzen R. et al., 2003, in Iye M., Moorwood A. F. M., eds, Proc. SPIE Conf. Ser. Vol. 4841, Instrument Design and Performance for Optical/Infrared Ground-based Telescopes. SPIE, Bellingham, p. 944

Malo L., Doyon R., Lafrenière D., Artigau É., Gagné J., Baron F., Riedel A., 2013, ApJ, 762, 88
Mamajek E. E., Hillenbrand L. A., 2008, ApJ, 687, 1264
Mamajek E. E., Meyer M. R., Hinz P. M., Hoffmann W. F., Cohen M., Hora J. L., 2004, ApJ, 612, 496
Marois C., Lafrenière D., Doyon R., Macintosh B., Nadeau D., 2006, ApJ, 641, 556
Masana E., Jordi C., Ribas I., 2006, A&A, 450, 735
Mason B. D., Wycoff G. L., Hartkopf W. I., Douglass G. G., Worley C. E., 2001, AJ, 122, 3466
Meshkat T., Kenworthy M. A., Quanz S. P., Amara A., 2014, ApJ, 780, 17
Meshkat T., Bailey V. P., Su K. Y. L., Kenworthy M. A., Mamajek E. E., Hinz P. M., Smith P. S., 2015, ApJ, 800, 5
Nielsen E. L. et al., 2012, ApJ, 750, 53
Pace G., 2013, A&A, 551, L8
Pearce T. D., Wyatt M. C., Kennedy G. M., 2015, MNRAS, 448, 3679
Pecaut M. J., Mamajek E. E., 2013, ApJS, 208, 9
Quanz S. P. et al., 2010, ApJ, 722, L49
Rajpurohit A. S., Reylé C., Allard F., Homeier D., Schultheis M., Bessell M. S., Robin A. C., 2013, A&A, 556, A15
Rameau J. et al., 2013, A&A, 553, A60
Rayner J. T., Cushing M. C., Vacca W. D., 2009, ApJS, 185, 289
Reggiani M., Meyer M. R., 2013, A&A, 553, A124
Reis W., Corradi W., de Avillez M. A., Santos F. P., 2011, ApJ, 734, 8
Rousset G. et al., 2003, in Wizinowich P. L., Bonaccini D., eds, Proc. SPIE Conf. Ser. Vol. 4839, Adaptive Optical System Technologies II. SPIE, Bellingham, p. 140
Schlegel D. J., Finkbeiner D. P., Davis M., 1998, ApJ, 500, 525
Schmidt S. J., West A. A., Bochanski J. J., Hawley S. L., Kielty C., 2014, PASP, 126, 642
Schröder C., Reiners A., Schmitt J. H. M. M., 2009, A&A, 493, 1099
Soderblom D. R., Stauffer J. R., Hudon J. D., Jones B. F., 1993, ApJS, 85, 315
Stauffer J. R., Hartmann L. W., Prosser C. F., Randich S., Balachandran S., Patten B. M., Simon T., Giampapa M., 1997, ApJ, 479, 776
Stephens D. C. et al., 2009, ApJ, 702, 154
Skrutskie M. F. et al., 2006, AJ, 131, 1163
Takeda G., Ford E. B., Sills A., Rasio F. A., Fischer D. A., Valenti J. A., 2007, ApJS, 168, 297
Thackrah A., Jones H., Hawkins M., 1997, MNRAS, 284, 507
Thies I., Pflamm-Altenburg J., Kroupa P., Marks M., 2015, ApJ, 800, 72
Tokovinin A., Mason B. D., Hartkopf W. I., 2010, AJ, 139, 743
Torres C. A. O., Quast G. R., Melo C. H. F., Sterzik M. F., 2008, in Reipurth B., ed., Handbook of Star Forming Regions, Volume II. Astron. Soc. Pac., San Francisco, p. 757
Valenti J. A., Fischer D. A., 2005, ApJS, 159, 141
van Leeuwen F., 2007, A&A, 474, 653
Voges W. et al., 1999, A&A, 349, 389
Wahhaj Z. et al., 2011, ApJ, 729, 139
White R. J., Gabor J. M., Hillenbrand L. A., 2007, AJ, 133, 2524
Wright J. T., Marcy G. W., Butler R. P., Vogt S. S., 2004, ApJS, 152, 261
Zuckerman B., Rhee J. H., Song I., Bessell M. S., 2011, ApJ, 732, 61

This paper has been typeset from a TEX/LATEX file prepared by the author.